Class II tetramer staining

Commercially available HLA Class II tetramers (Beckman Coulter) conjugated to PE were combined with dominant HIV epitopes (DRB1*0101-DRFYKTLRAEQASQEV, DRB1*0301- PEKEVLVWKFDSRLAFHH, DRB1*0401-DRFYKTLRAEQASQEV, DRB1*1501- PEKEVLVWKFDSRLAFHH) and used to stain PBMC (20 min at 37 ºC, 5% CO2). Tetramer+ cells were subsequently enriched on magnetic columns (Miltenyi Biotec), as previously described (Day *et al, J Clin Invest* 2003). After recovery of the tetramer-enriched fraction, surface staining for PD-1, CD3, CD4, CD8, CD14 and CD19 was completed. Exclusion channels for dead cells (blue viability dye, Invitrogen), CD8, CD14 and CD19 were used to gate out unwanted events, as described for ICS.

Edu incorporation assay

In order to validate the CFSE proliferation measurements we used a second method based on EdU (5-ethynyl-2'-deoxyuridine) incorporation to DNA during active DNA synthesis. Briefly, 2 x 10^6 CD8 depleted PBMC's were stimulated with HIV gag peptide pool or CMV lysate and CMV pp65 peptide pool, or PHA. Cells were pulsed with 10 μM Click-iT™ EdU (Invitrogen) for 6 hours prior to collection at 48, 72 and 96 hours after stimulation and stained with antibodies against CD14-CD19 (excluded population), CD3, CD4, CD8. After fixation and permeabilization cells were stained with Alexa Fluor® 488 azide according to the manufacturer's instructions. Stained cells were analyzed by flow cytometry on a 5 laser LSR Fortessa (BD Bioscience).

Cell death analysis

In order to evaluate the impact of PD-L1 blockade on cell death a combined ICS/CFSE was performed as in the method section of the main text. Cells were also stained with an antibody against active caspase-3 (clone C92-605, BD Biosciences) in order to measure apoptotic cells and a dead cell viability dye to evaluate necrotic cells (blue viability dye; Invitrogen). Cells were also counted with a Guava counter instrument (Millipore) to evaluate the total cell number and total cell death.

PD-L1 surface expression

After the thawing of cryopreserved samples, cells were immediately incubated for 10 minutes with Fc receptor blocking reagent (Miltenyi) and subsequently stained for CD3, CD4, CD8, CD56, CD14, CD19 and PD-L1 (clone MIH1, BD Bioscience) as described in the methods section of the main text.

Table S1. Primer sequences for qPCR

Figure S1. Blockade of the PD-1 pathway can restore IL-21 mRNA levels. mRNA levels of IL-21 after GAG stimulation and blockade with PD-L1 antibody or isotypic control in CP (n=10), were measured by qRT-PCR and normalized to the housekeeping gene GAPDH.

Figure S2. PD-1 is pre-expressed on HIV-specific CD4 T cells and not significantly altered in the 6 hours following encounter with the cognate antigen. A) Comparative PD-1 levels on HIV-specific Class II tetramer+ CD4 T cells (filled trace) and in the general CD4 T cell population (open trace) of two HIV-infected subjects, in the absence of pre-stimulation with synthetic peptide. B) Resting HIV-specific CD4 T cells identified by Class II tetramers in PBMC express significantly higher levels of PD-1 than the general CD4 T cell population (n=12; Wilcoxon signed rank test). C-D) Comparative PD-1 levels on HIV-specific Class II-tetramer+ CD4 T cells before stimulation, after a 6-hour stimulation with the cognate epitope, and after a 6-hour stimulation with the epitope in the presence of brefeldin A. C) Representative example of one of the subjects investigated. D) Summary data on four individuals.

Figure S3. PD-1 is pre-expressed on HIV-specific T cell subsets. A) Comparison of PD-1 expression (MFI) on HIV Gag-specific CD4 T cells producing IL-2+ alone, IL-2 and IFN-γ, or IFN-γ alone after encounter with the cognate antigen, in the same individuals (n=22). Statistical comparisons were made with the Friedman test

followed by Dunn's post tests for pair-wise comparisons. B) Correlation of PD-1 expression (MFI) on HIV Gag-specific CD8 and CD4 T cells of 41 subjects (Spearman).

Figure S4. Distribution of HIV-specific CD4 T cells according to their differentiation status. ICS was performed on PBMCs stimulated with HIV Gag peptides. CD4 T cell were characterized according to their differentiation status using CD27 and CD45RA expression (Naïve: CD27 high CD45RA high, central memory:CD27 high CD45RA low, effector-memory:CD27 low CD45RA low, terminal effector: CD27 low CDRA high); A) Distribution of IFN-γ+ HIV-specific CD4 T cells from patients with different disease status; B I-II) Comparison of the IFN-γ+ HIV-specific CD4 T cells, found in the central memory (I) and effector memory (II) differentiation subsets, between patients with different disease status; C-D) Distribution of PD-1 expressing IFN-γ+ HIV-specific CD4 T cells in the central memory and effector memory subsets.

Figure S5. Expression of PD-L1 on different cell subsets from HIV-infected individuals with different disease status. A) Percentage of PD-L1 positive cells (I) and expression of PD-L1 (II) (MFI) in different cell subsets; B) Comparison of the percentage of PD-L1 expressing cell subsets in patients with different disease status.

Figure S6. Measurements of CD4 T cell proliferation by EDU incorporation compared to CFSE dilution. A-C) Kinetic analysis of proliferation using CFSE staining (I) and EDU (II) incorporation assays. CD8 depleted PBMCs were either left unstimulated (A) or were stimulated with HIV Gag peptide (B) or CMV lysate (C).

Figure S7. Impact of PD-L1 blockade on cell death. CD8-depleted PBMCs were stimulated with HIV GAG peptide pools in the presence of PD-L1 blocking

antibody or isotypic control. A) Percentage of dead cell as measured by Guava counter instrument; B) Percentage of dead cells measured using a viability dye and analyzed with flow cytometry; C) Percentage of CD4 T cells that have high levels of activated Caspase-3. ICS performed on the same assays did not show a significant population of HIV-specific CD4 T cells co-expressing IFN-γ and activated caspase 3 (not shown).

Figure S8. Co-expression of CTLA-4 with PD-1, CD160 and CD244 on HIV-specific CD4 T cells. ICS was performed on PBMC stimulated with HIV Gag peptide pools, with replacement of the LAG-3 antibody used in Fig 5 by an anti-CTLA antibody (intracellular staining). Co-expression patterns PD-1, 2B4, CD160 and CTLA-4 on IFN-γ-producing CD4 and CD8 T cells (n=8).

Figure S9. Phenotypic analysis of 2B4, CD160 and LAG-3 expression on HIV-specific IFN-γ+ CD4 and CD8 T cells expressing intermediate or high levels of PD-1. ICS was performed on PBMC stimulated with HIV Gag peptides. A-B) I) CD4 and CD8 T cells gated according to their level of PD-1 expression into PD-1^{low}, PD-$1^{intermediate}$ and PD-1^{high} subsets; II-IV) Frequency of PD-1, 2B4 and CD160 on PD-$1^{intermediate}$ and PD-1^{high} expressing IFN-γ-producing CD4 and CD8 T cells (n=9).

Figure S10. Similarities and differences in co-inhibitory molecule expression on HIV- and CMV-specific T cells. A- B) Proportions of virus-specific T cells identified by IFN-γ ICS that simultaneously expressing one, two, three of four inhibitory molecules. Expression patterns of individual inhibitory molecules on virus-specific CD4 (C) and CD8 (D) T cells.

Table S1. Primer sequences for the qPCR

Primers name	Forward Primer	Reverse Primer
IL-2	TGCAACTCCTGTCTTGCATTG	GGCCTTCTTGGGCATGTAAA
IFN-γ	CGAGATGACTTCGAAAAGCTGA	TCTTCGACCTCGAAACAGCA
IL-13	CGGTCATTGCTCTCACTTGC	CACGTTGATCAGGGATTCCA
GAPDH	TCATCATCTCTGCCCCCTCT	AGTGATGGCATGGACTGTGG
IL-21	CATGGAGAGGATTGTCATCTGTC	CAGAAATTCAGGGACCAAGTCAT

Figure S1. Blockade of the PD-1 pathway can restore IL-21 mRNA levels

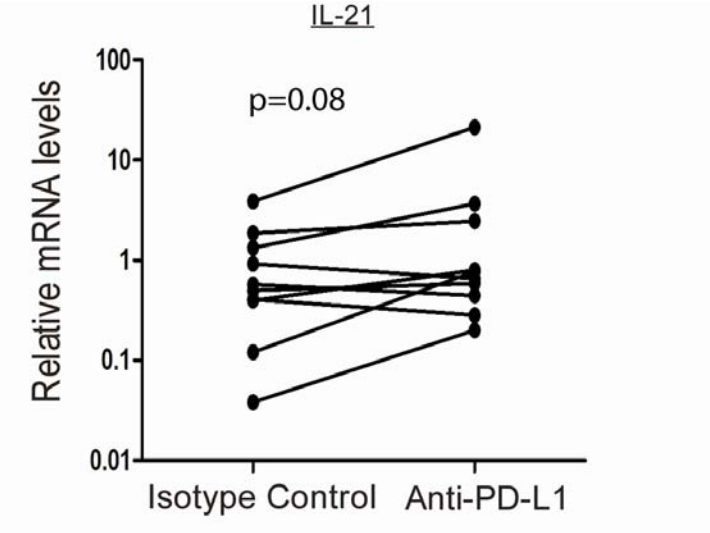

Figure S2. PD-1 is pre-expressed on HIV-specific CD4 T cells and not significantly altered in the 6 hours following encounter with the cognate antigen

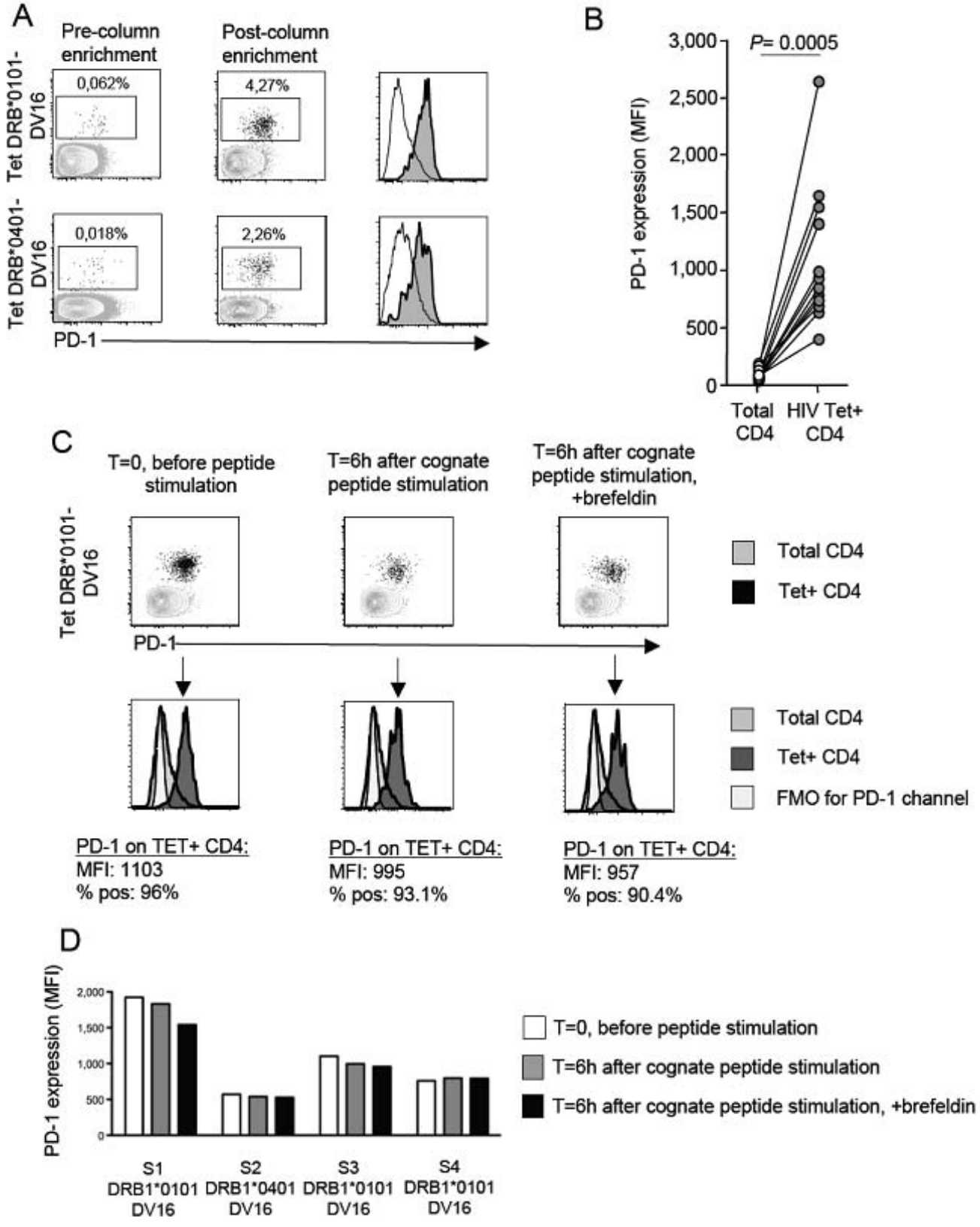

Figure S3. PD-1 expression on HIV-specific T-cell subsets

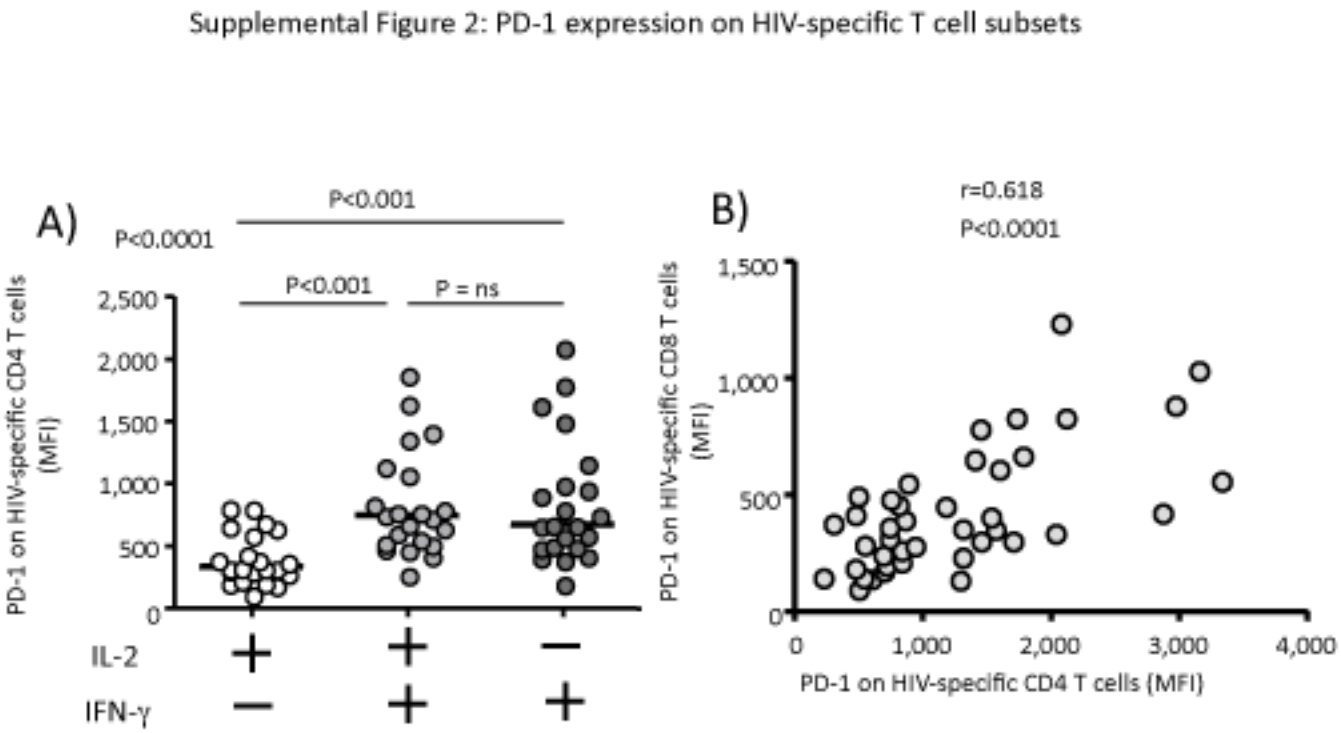

Figure S4. Distribution of HIV-specific CD4 T cells according to their differentiation status

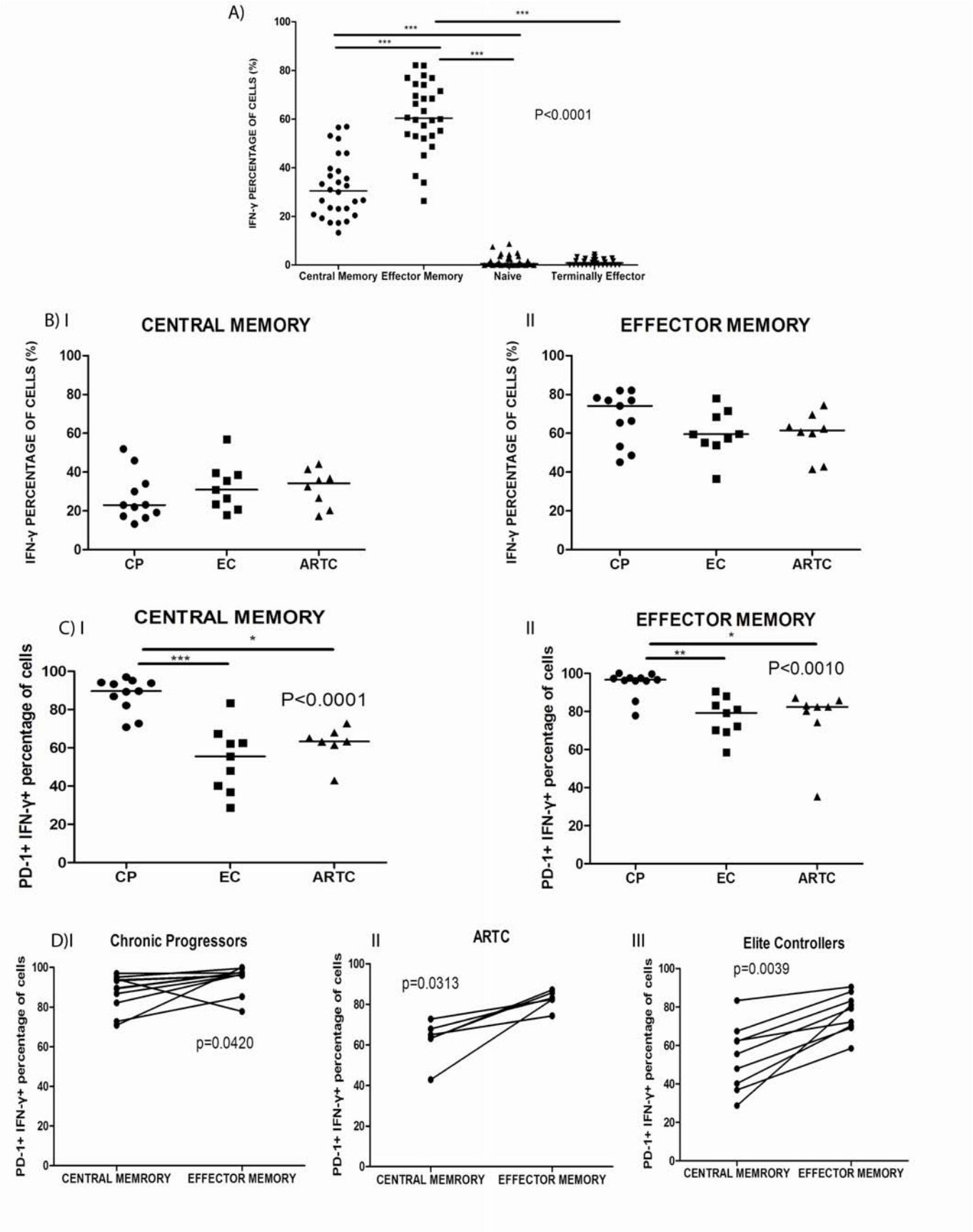

Figure S5. Expression of PD-L1 on different cell subsets from HIV-infected individuals with different disease status

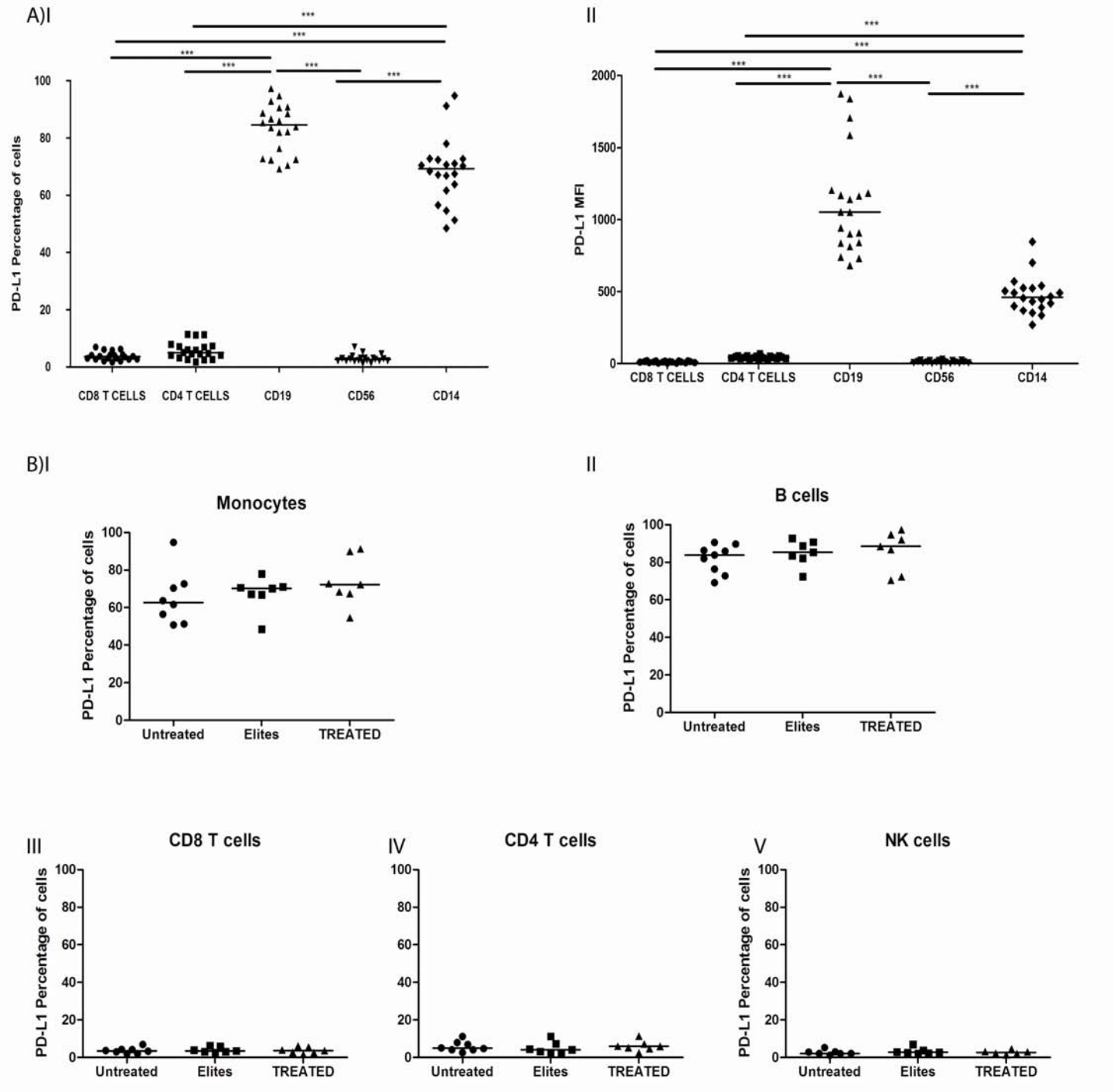

Figure S6. Measurement of CD4 T-cell proliferation by EDU incorporation compared to CFSE

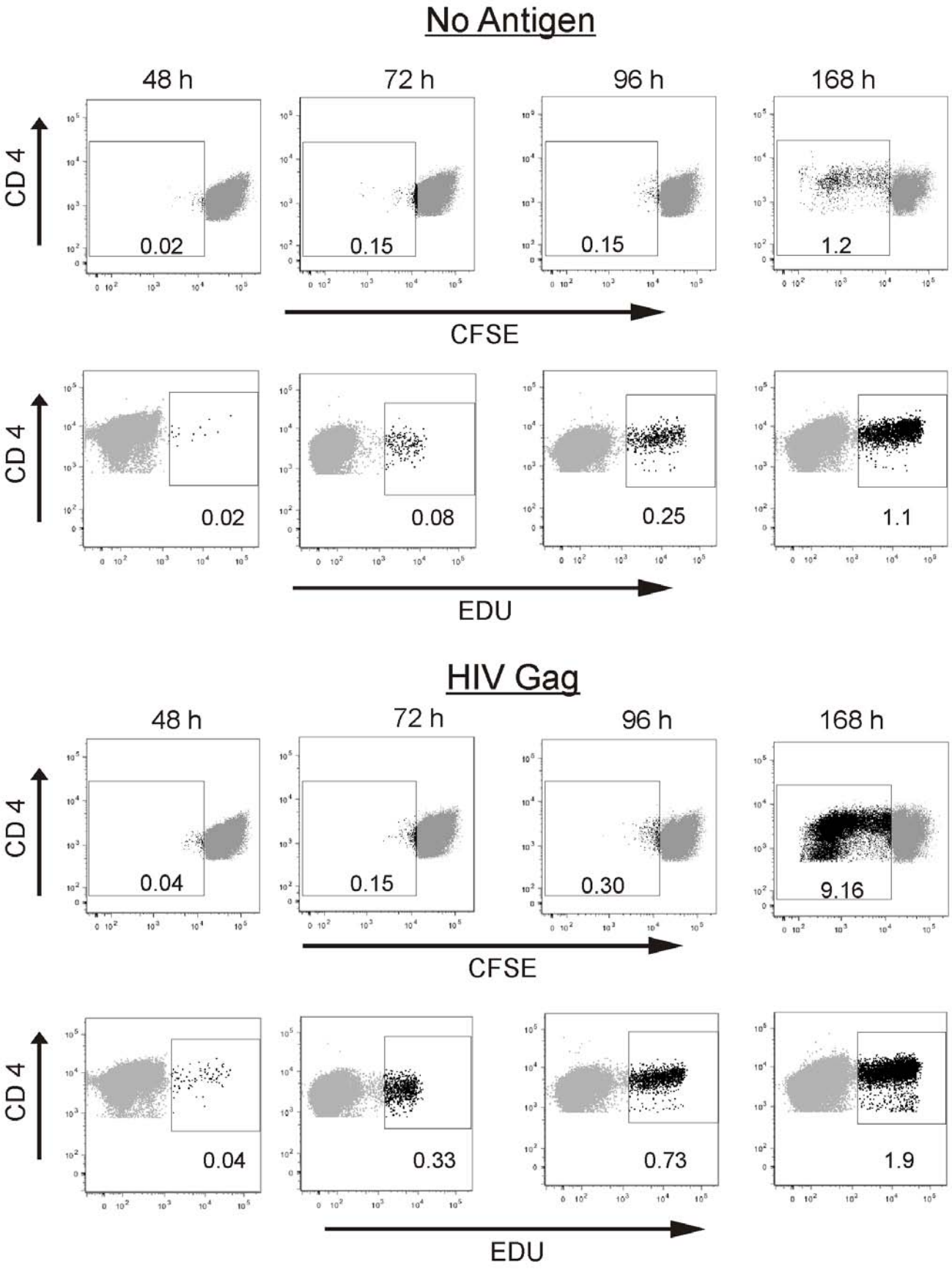

Figure S7. Impact of PD-L1 blockade on cell death

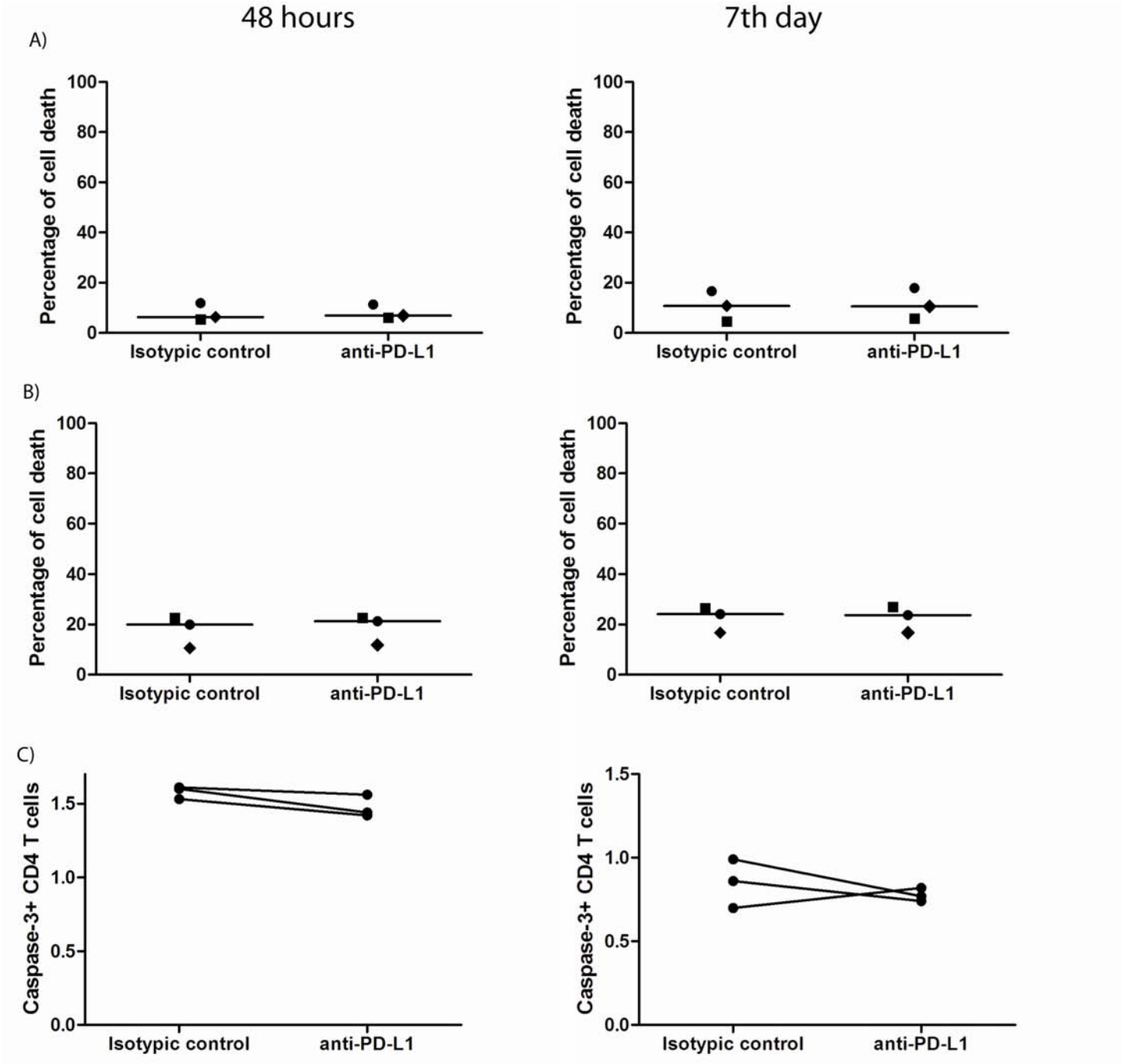

Figure S8. Co-expression of CTLA-4 with PD-1, CD160 and CD244 on HIV-specific CD4 T cells

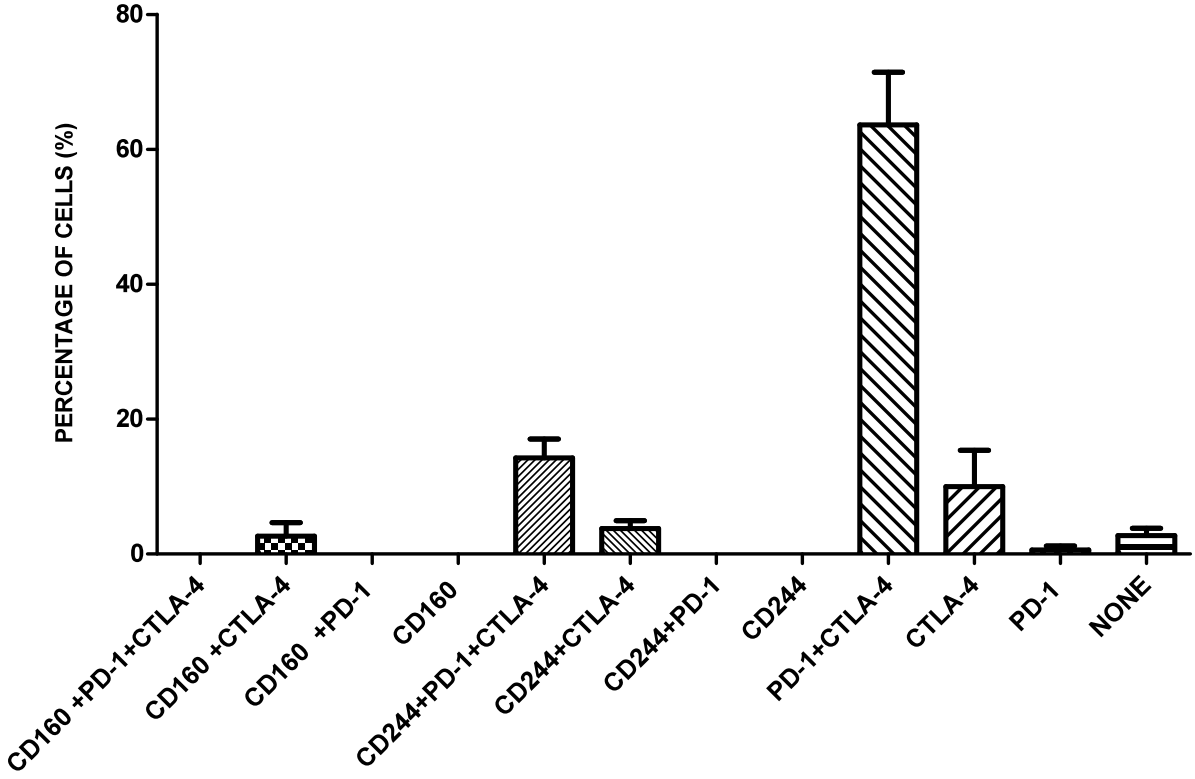

Figure S9. Phenotypic analysis of the 2b4, CD160 and LAG-3 percentage of cells within the PD-1 intermediate and the PD-1 high expressing HIV-specific IFN-g CD4 and CD8 T cells

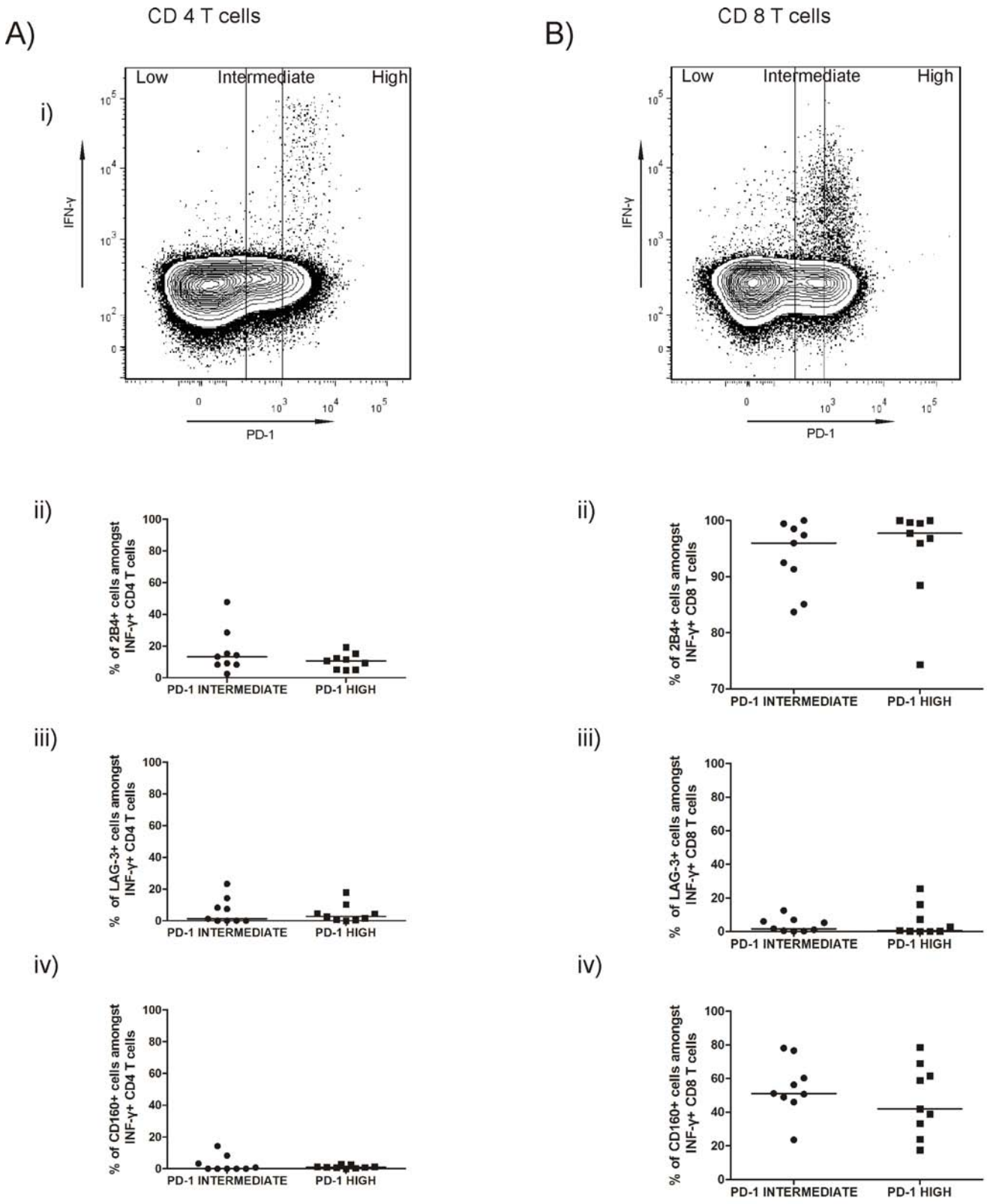

Figure S10. Similarities and differences in co-inhibitory molecule expression on HIV- and CMV-specific T cells